Research of Large Field of View Scan Mode for Industrial CT

FU Jian, LU Hong-nian

(*School of Mechanical Engineering and Automation, Beijing University of Aeronautics and Astronautics, Beijing 100083, China*)

Abstract: For industrial computed tomography systems, generation II scan mode has a large field of view but time-consuming and generation III has a small field of view but fast. In order to realize the rapid ICT test of large objects, a scan mode based on generation III called large field of view scan was discussed and its reconstruction algorithm based on FBP was deduced. The validity of the algorithm was verified by the results of computer simulation and experiments. Analysis showed that the effective scan field of view could be improved by more than 90% compared with that of generation III.

Key words: industrial computed tomography; fan beam scan; filter back-projection algorithm; rebin algorithm; non-destructive testing

工业 **CT** 大视场扫描成像方法研究. 傅健, 路宏年. 中国航空学报(英文版). 2003, 16(1): 59-64.

摘 要: 工业 CT 二代扫描方式扫描视场大, 但扫描时间长; 三代扫描方式扫描时间短, 但扫描视场小。为解决较大尺寸构件 ICT 快速检测问题, 讨论了一种基于三代扫描的大视场扫描方式, 推导了它的 FBP 重构算法。计算机模拟和实验结果证明了该算法的正确性。分析表明, 其有效扫描视野在三代的1.9倍以上。

关键词: 计算机层析成像; 扇束扫描; FBP 算法; 重排算法; 无损检测

文章编号: 1000-9361(2003)01-0059-06 中图分类号: TP391 文献标识码: A

Industrial computed tomography (ICT) is a novel non-contacted measurement technology. Based on the high-resolution, high-contrast images generated by X-ray scan and reconstruction, it can permit an exact measurement of the position and the dimensions of the internal structure of many industrial components and provide information that cannot currently be provided nondestructively by any other means[1]. The measurement of the wall thickness of air engine blades is a good example.

The majority of scan modes currently adopted by ICT systems can be classified into two classes: generation II or TR and generation III or RO. The feature of TR is that the objects need to rotate and transverse. The feature of RO, depicted in Fig. 1 (a), is that the objects only rotate. Although RO needs less scan time than TR, large objects have to employ TR because of the limits caused by the effective angle of the X-ray beam and the length of detectors. It results in a slice scan with no less than 10min.

In order to overcome this difficulty, a scan mode called large field of view (LFOV) based on RO is proposed and depicted in Fig. 1(b). Based on the rebin reconstruction algorithm of the fan beam, the algorithm for LFOV is presented. The results of computer simulation and experiments verify the validity of this scan mode.

1 LFOV Scan Mode

Fig. 1(c) shows the scan principle. S_0 is the X-ray source. D_1D_2 represents the linear array de-

Received date: 2002-06-27; Revision received date: 2002-12-16
Article URL: http://www.hkxb.net.cn/cja/2003/01/0059/

tector (LDA). δ is the effective angle of the X-ray beam. D is the distance from the X-ray source to the detectors. $S_0D_1D_2$ is the scan geometry of RO. RO can inspect the objects with the radius no larger than r_1 as long as the objects rotate 360° at the point O_1.

For LFOV, the scan geometry does not change and the rotation center of the table moves to O_2. The objects with the radius no larger than r_2 can be tested when they rotate 360°. The data collected by the actual detector D_1D_2 can be converted into the data collected by the virtual detector AB through rebin and interpolation.

Without changing the position and the length of the detector D_1D_2 and the angle of the X-ray fan beam, the LFOV scan mode can test the large objects that are usually inspected with the detector AB and the angle of the X-ray beam as twice as that in RO.

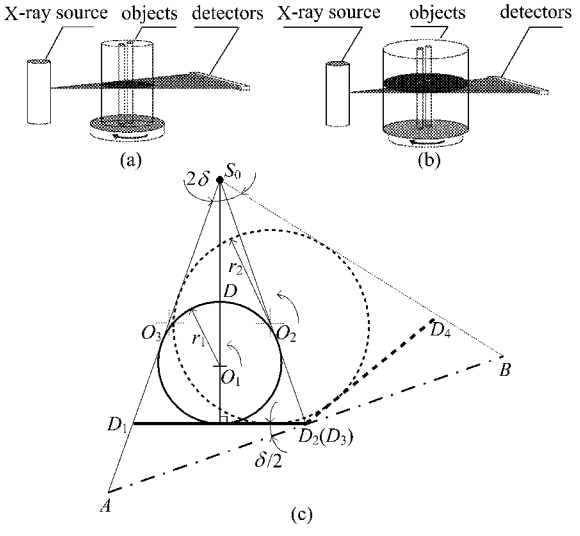

Fig. 1 LFOV scan principle

2 Algorithm for LFOV

There exist reconstruction formulas for the parallel beam and fan beam[2,3]. The reconstructed slice is represented by $a(r,\theta)$ in polar coordinates.

$$a(r,\theta)=\int_0^{\pi}h(x_r)*p(x_r,\varphi)\big|_{x_r=r\cos(\theta-\varphi)}\,d\varphi=\int_0^{\pi}g[x_r,\varphi]\big|_{x_r=r\cos(\theta-\varphi)}d\varphi \qquad (1)$$

where $h(x_r)$ is a filter function. $p(x_r,\varphi)$ is the projection of the parallel beam. The formation of the projection is depicted in Fig. 2(b).

$$a(r,\theta)=\int_0^{2\pi}\frac{1}{U^2}\tilde{p}_e(s_1,\beta)\,d\beta \qquad (2)$$

where $U=\dfrac{D+r\sin(\beta-\theta)}{D}$ is a weighting factor. $p(s,\beta)$ is the projection of the fan beam. $p_e(s,\beta)=p(s,\beta)\dfrac{D}{\sqrt{D^2+s^2}}$ is the weighted projection. $g(s)=\dfrac{1}{2}h(s)$ is a filter function. $\tilde{p}_e(s,\beta)=p_e(s,\beta)*g(s)$ is the filtered projection. $s_1=\dfrac{Dr\cos(\beta-\theta)}{D+r\sin(\beta-\theta)}$ is the position of the reconstructed point. The formation of the projection of the fan beam is described in Fig. 2(a).

The mission of the reconstruction algorithm for the LFOV presented by this paper is to solve how to reconstruct the object with the radius r_2 using the detector D_1D_2. The conventional filter back projection (FBP) algorithm for the fan beam described by Eq. (2) needs the complete fan beam projections for 360°. Obviously, LFOV can not acquire the complete fan beam projections for 360°. So this algorithm can not be used directly. The incomplete projections need to be rebinned or reorganized. This idea of rebin comes from two characteristics of parallel beam projections implied in Fig. 2(b). One is that the projections from 0° to 180° are the same as those from 180° to 360°. Another is that the projection does not change when the projecting direction is converse.

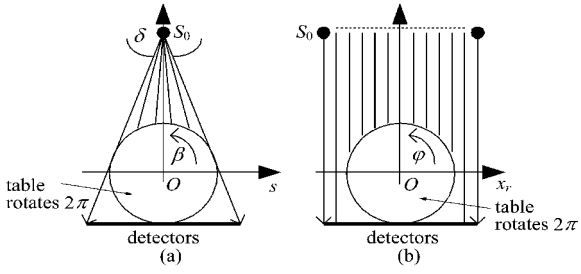

Fig. 2 Two kinds of scan modes

The principle of the LFOV algorithm based on the above idea is to convert the incomplete projections of the fan beam collected by the actual detector D_1D_2 into the equivalent complete projec-

tions of the fan beam collected by the virtual detectors AB. Fig. 3 is the processing chart of the LFOV algorithm presented by this paper.

According to the arrangement of detector channels, there are two kinds of rebin algorithms converting fan beam projections into parallel beam projections: equivalent space and equivalent angle. The algorithm for an equivalent angle is described in Ref. [4]. This part will firstly show the algorithm for the equivalent space. Then an LFOV reconstruction algorithm is presented.

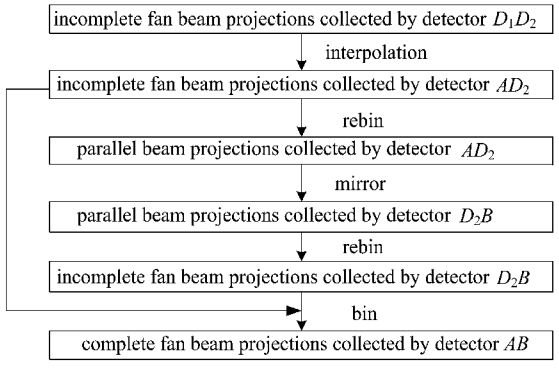

Fig. 3 Reconstruction flow for LFOV

2.1 Rebin algorithm for equivalent space fan beam

The essential to convert fan beam projections $p(s,\beta)$ into parallel beam projection $p(x_r,\varphi)$ is to construct a transform between two address spaces: (s,β) and (x_r,φ).

Fig. 4 depicts the geometry relationship between the fan beam ray and parallel beam ray under a certain projection angle. The relationships among these parameters of the fan beam and parallel beam implied in Fig. 4 can be expressed as

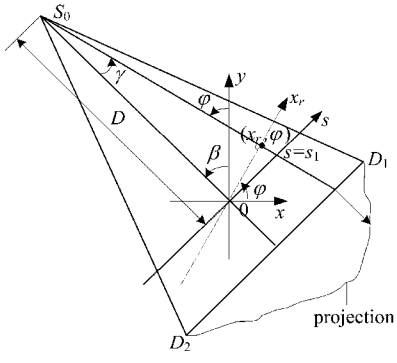

Fig. 4 Geometry relationship of parameters of equivalent space fan beam ray

$$\varphi = \beta + \gamma = \beta + \arctan(s/D),$$
$$x_r = s\cos\gamma = sD/\sqrt{D^2+s^2}$$

Based on the above equations, Fig. 5 depicts the transform between the two address spaces: (s,β) and (x_r,φ). Every point of intersection is the position of a ray. The point of intersection of the solid lines is the address storing the fan beam projection. The point of intersection of the dot lines is the address storing the parallel beam projection. The point of intersection of the dot lines is what this paper needs to calculate.

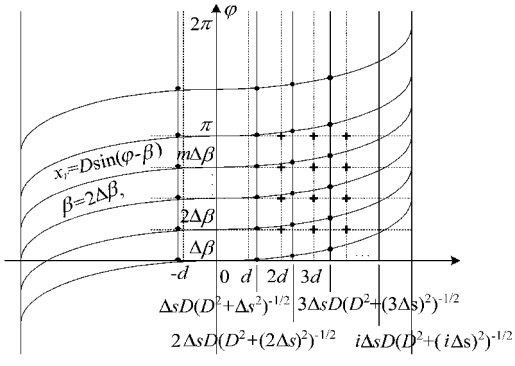

Fig. 5 Transform between space (s,β) and (x_r,φ)

From Fig. 5, one can know that it is possible to get the address storing the parallel projections denoted by the point of intersection of the dot lines in virtue of the interpolation of the position of the point of intersection of the solid lines vertically and horizontally. x_r, φ, β and s are discretized. $p(s,\beta)$ and $p(x_r,\varphi)$ are represented by $p(i\Delta s, j\Delta\beta)$ and $p(n\Delta x_r, m\Delta\varphi)$. They are simplified to $p(i,j)$ and $p(n,m)$. There are interpolation results as follows (linear interpolation)

$$p(i,m) = (1-\delta_j)p(i,j) + \delta_j p(i,j+1)$$
$$p(n,m) = (1-\delta_i)p(i,m) + \delta_i p(i+1,m)$$
$$\delta_j = (m - \arctan(i\Delta s/D)/\Delta\beta) - \mathrm{Int}[m - \arctan(i\Delta s/D)/\Delta\beta]$$
$$\delta_i = \sqrt{n^2d^2D^2/(D^2-n^2d^2)} - \mathrm{Int}[\sqrt{n^2d^2D^2/(D^2-n^2d^2)}]$$

Where Int[] is the integer part.

From the above equations, the parallel projections can be calculated based on the fan beam projections collected by the detector AD_2. This algorithm can be also used to get the fan beam projections from parallel beam projections conversely.

2.2 LFOV rebin reconstruction algorithm

Following the algorithm illustrated in Fig. 3, it is necessary to transform the projections collected by the detector the D_1D_2 to the detector the AD_2. A method is linear interpolation. The interpolation formulas as follows can be deduced from the geometry relationship between D_1D_2 and AD_2.

$$\left.\begin{aligned} t &= s/\cos(\delta/2) \\ p(s,\beta) &= p(\mathrm{Int}[t],\beta) + (t - \mathrm{Int}[t]) \cdot \\ &\quad (p(\mathrm{Int}[t]+1,\beta) - p(\mathrm{Int}[t],\beta)) \end{aligned}\right\} \quad (3)$$

Then the fan beam projections collected by the detector AD_2 are rebinned into parallel beam projections using the algorithm described in 2.1.

The following step is to mirror the parallel beam projections for 360 ° to the projections collected by the detector BD_2 in virtue of the symmetry of the parallel beam that $p(x_r, \varphi) = p(-x_r, \varphi \pm \pi)$.

The algorithm in 2.1 is conversely used again to convert the parallel beam projections collected by the detector BD_2 into corresponding fan beam projections.

Finally the equivalent and complete fan beam projections for 360 ° collected by the detector AB can be created by connecting the fan beam projections collected by the detectors AD_2 and BD_2. Now the conventional algorithm for fan beam in Eq. (2) can be used to reconstruct the image.

3 Computer Simulation

In order to verify the LFOV scan mode and its reconstruction algorithm, a model shown in Fig. 6 is used. Table 1 gives the parameters of the model. The simulation conditions are (unit: pixel):

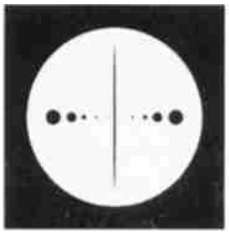

Fig. 6 Simulation model

the distance from X-ray source to rotation center D: 800; the number of detector channels: 360; the size of the reconstruction image: 360 × 360; the number of views: 360.

The equivalent ray beam angle is 13 °. Fig. 7 shows LFOV projections processing flow and reconstruction image.

Table 1 Geometry parameters of the model

ellipse	origin position		half of the length of axis		attenuation coefficient
	X	Y	long axis	short axis	
1	0	0	144	144	1500
2	0	0	120	1.5	1000
3	− 10	0	1	1	1000
4	10	0	1	1	1000
5	− 30	0	2	2	1000
6	30	0	2	2	1000
7	− 50	0	4	4	1000
8	50	0	4	4	1000
9	− 70	0	8	8	1000
10	70	0	8	8	1000
11	− 100	0	12	12	1000
12	100	0	12	12	1000

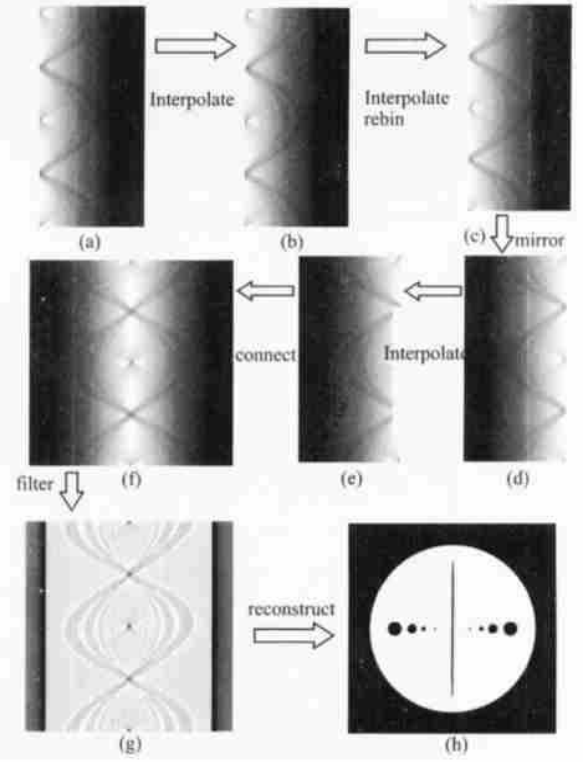

Fig. 7 LFOV projections processing flow and reconstruction image

(a) 180 × 373 original fan beam projections; (b) fan beam projections resulting from Eq. (3); (c) 180 × 360 equivalent parallel beam projections for 360 ° resulting from the algorithm in 2.1; (d) 180 × 360 equivalent parallel beam projections for 360 ° collected by detector BD_2; (e) 180 × 360 equivalent fan beam projections for 360 ° collected by detector BD_2 resulting from the algorithm in 2.1; (f) 360 × 360 fan beam projections for 360 ° collected by detector AB resulting from the connecting in 2.2; (g) filtered projections; (h) fan beam reconstruction image

4 Performance Analysis

This part makes a research about the precision of the LFOV scan mode and its reconstruction algorithm.

The model in Fig. 6 is simulated and reconstructed respectively by fan beam RO, parallel beam and LFOV. The reconstruction images are compared with the model. Regularized mean square distance, regularized mean absolute distance and the worst distance are the estimation standards of performance[2]. The results are illustrated in Fig. 8 and Table 2.

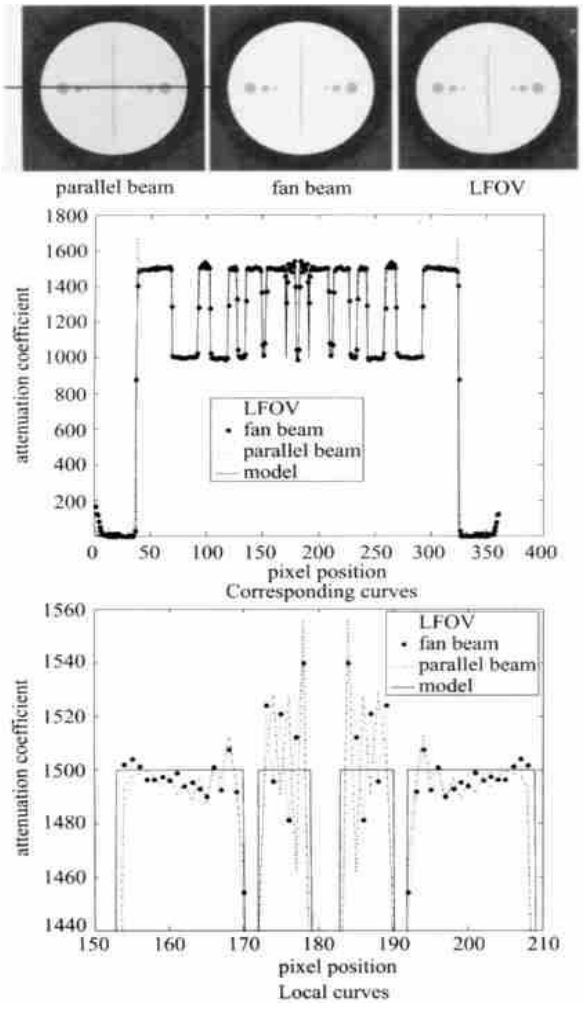

Fig. 8 Comparison between the images reconstructed by parallel beam, fan beam and LFOV

Table 2 Image quality parameters

	mean square distance	mean absolute distance	worst distance
parallel beam	0.0397	0.0078	245.2013
fan beam	0.0407	0.0081	299.6062
LFOV	0.0402	0.0091	330.8535

Additionally, noise with the standard deviation 1% is added into the projections. The signal noise ratio of the reconstruction images is calculated to evaluate the anti-noise performance of the algorithms. The results are illustrated in Fig. 9 and Table 3.

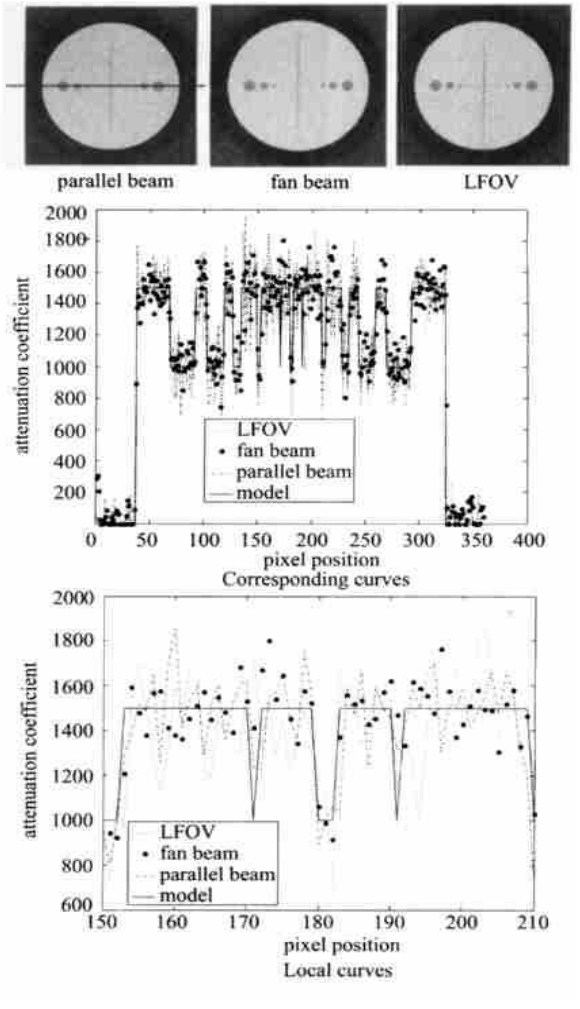

Fig. 9 Comparison in anti-noise performance between parallel beam, fan beam and LFOV

Table 3 SNR of reconstruction images

parallel beam	fan beam	LFOV
14.13	14.02	14.82

The above results show that the LFOV scan mode and its reconstruction algorithm are right.

5 Experiments

The LFOV scan mode and its algorithm are verified by the experiments using ACTIS-450/600 ICT system of BIR Corp. and DR/ICT-320/400 ICT system of Beijing University of Aeronatics and

Astronautics with the blade of a jet engine as the object. Fig. 10 is the reconstruction image of a slice of the object.

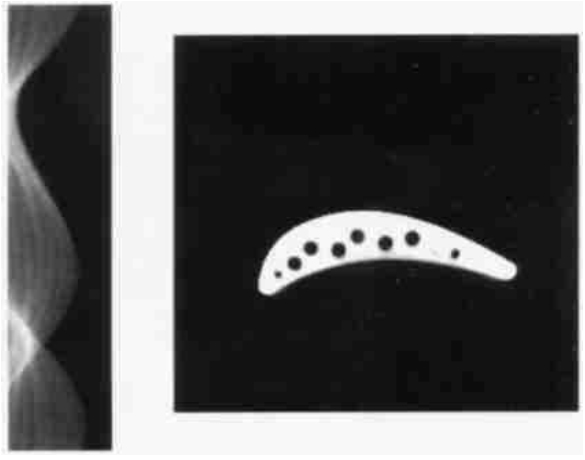

Fig. 10 LFOV image of the blade of jet engine
(a) original projection; (b) reconstruction image

6 Effective Scan View Analysis

From Fig. 1(c), the maximum size of scan view for RO is r_1 when the detector D_1D_2 remains its length. Under the same conditions, the maximum size of scan view for LFOV is r_2. The geometry relationship implied in Fig. 1 can be expressed as

$$r_2 = D/(1 + 1/(2 \times r_1/(D - r_1)))$$

For ICT systems, the value of D lies from 950mm to 1000mm. When D is 950mm and r_1 is 100mm, r_2 equals 190mm and r_2/r_1 equals 1.9. When D is 1000mm and r_1 is 100mm, r_2 equals 200mm and r_2/r_1 equals 2. Obviously, the LFOV scan mode can improve the effective scan field of view by more than 90% compared with that of RO.

7 Conclusions

When the table rotates 360° at the points O_1 and O_2 respectively, the projections collected by the detector D_1D_2 can be rebinned into complete fan beam projections for 360° in virtue of another technology developed by the authors.

The results of computer simulation and experiments verify the validity of the LFOV scan mode and its reconstruction algorithm. Because there exist several interpolation steps, the precision of this algorithm is, to some extent, limited.

This kind of scan mode is beneficial to the rapid test of large objects when the requirement of the precision is medium.

References

[1] E1441-00, Standard guide for computed tomography (CT) imaging[S]. ASTM, 2000.

[2] Herman G T. Image reconstruction from projection: the fundamentals of computed tomography[M]. New York: Academic Press, 1980.

[3] Kak A C, Malcolm S. Principles of computerized tomographic imaging[M]. New York: IEEE Press, 1999.

[4] 庄天戈. CT 原理与算法[M]. 上海: 上海交通大学出版社, 1992.
Zhuang T G. CT principle and algorithm [M]. Shanghai: Shanghai Jiao tong University Press, 1992. (in Chinese)

Biography:

FU Jian Born in 1976, he received B.S. from Beijing University of Aeronautics and Astronautics in 1999. He is studying for his doctoral degree in BUAA. Since 1999, he has done research work on industrial digital radiology and computed tomography. He has published some relative papers in various periodicals. Tel: (010) 82317867, E-mail: fujian706@263.net